Thyroid follicle development requires Smad1/Smad5- and endothelial-dependent basement membrane assembly

Mylah Villacorte[1†], Anne-Sophie Delmarcelle[1†], Manon Lernoux[1], Mahé Bouquet[1], Pascale Lemoine[1], Jennifer Bolsée[1], Lieve Umans[2,3], Susana Chuva de Sousa Lopes[5], Patrick Van Der Smissen[1], Takako Sasaki[6], Guido Bommer[1], Patrick Henriet[1], Samuel Refetoff[7], Frédéric P. Lemaigre[1], An Zwijsen[2,4], Pierre J. Courtoy[1], and Christophe E. Pierreux[1*]

[1] de Duve Institute and Université catholique de Louvain, Brussels, Belgium, [2] VIB Center for the Biology of Disease, KU Leuven, Belgium, [3] Laboratory of Molecular Biology (Celgen), Stem Cell Biology and Embryology, KU Leuven, Belgium, [4]Department of Human Genetics, KU Leuven, Belgium, [5]Department of Anatomy and Embryology, Leiden University Medical Center, Leiden, The Netherlands, [6]Department of Matrix Medicine, Faculty of Medicine, Oita University, Oita, Japan, [7]Department of Medicine, Pediatrics and Genetics, The University of Chicago, Chicago, IL, USA.

† Equally contributing first authors

*corresponding author. Fax : +32 2 764 75 43

E-mail address: christophe.pierreux@uclouvain.be

Keywords:

Thyroid, Smad1/5, follicles, epithelium, extracellular matrix

Summary

Epithelial BMP-Smad1/5 signaling and associated endothelial cells are required for reorganization of thyroid progenitor cell mass into mature follicles via deposition of basement membrane proteins.

Abstract

Thyroid follicles, the functional units of the thyroid gland, are delineated by a monolayer of thyrocytes resting on a continuous basement membrane. Developmental mechanisms whereby follicles are formed by reorganization of a non-structured mass of non-polarized epithelial cells (folliculogenesis) largely unknown. Here we show that assembly of the epithelial basement membrane is critical for folliculogenesis and is controlled by endothelial cell invasion and by BMP-Smad signaling in thyrocytes. Thyroid-specific double Smad1 and Smad5 knockout mice (Smad1/5^{dKO}) displayed growth retardation, hypothyroidism and defective follicular architecture. In Smad1/5^{dKO} embryonic thyroids, epithelial cells remained associated in large clusters and formed small follicles. Although similar follicular defects are found in Vegfa^{KO} thyroids, Smad1/5^{dKO} thyroids had normal endothelial cell density yet impaired endothelial differentiation. Interestingly, both Vegfa^{KO} and Smad1/5^{dKO} thyroids displayed impaired basement membrane assembly. Furthemore, conditioned medium (CM) from embryonic endothelial progenitor cells (eEPC) rescued the folliculogenic defects of both Smad1/5^{dKO} and Vegfa^{KO} thyroids. Laminin $\alpha1\beta1\gamma1$, abundantly released by eEPC into CM, was critically required for folliculogenesis. Thus, epithelial Smad signaling and endothelial cell invasion promote folliculogenesis via assembly of the basement membrane.

Introduction

Thyroid follicles are the functional units of the thyroid gland. Each follicle is composed of a polarized monolayer of epithelial cells delineating a close lumen where thyroglobulin (TG) is stored as colloid. Thyrocytes differentiate from thyroid progenitors that bud from the foregut endoderm as a mass of non-polarized epithelial cells, which reorganize to form pre-follicular structures by acquisition of apico-basal polarity (Fagman et al., 2006; Hick et al., 2013). Differentiated thyrocytes face the lumen at the apical pole, and are attached to the basement membrane at their basal pole. In the mature thyroid, a dense network of blood vessels surrounds each follicle. Together, they form angio-follicular units responsible for T_3 and T_4 thyroid hormone synthesis and storage within TG, and then hormone secretion into the bloodstream (Colin et al., 2013; Nilsson and Fagman, 2013). A limited number of transcription factors (Nkx2.1, Pax8, Foxe1 and Hhex) and signalling molecules are known to control thyroid development (Fagman and Nilsson, 2010), but the molecular and subcellular morphogenetic machineries regulating follicle formation remain essentially unknown.

Several studies have demonstrated the importance of epithelial-endothelial interactions in organs developing from the endoderm (Hick et al., 2013; Lammert et al., 2001; Lazarus et al., 2011; Pierreux et al., 2010). In the thyroid, we found that endothelial cells are recruited in response to epithelial-derived VEGFa and are essential for the organization of thyroid epithelial cell mass into follicles (Hick et al., 2013). However, the identity and mode of action of folliculogenic factor(s) are still unknown.

Bone/body morphogenetic proteins (BMP) are members of the transforming growth factor (TGF-β) family that control many developmental processes such as epithelial differentiation and tissue morphogenesis (Macias et al., 2015). Upon BMP ligand binding to its receptor, the intracellular signal transducers, Smad1/5/8, become activated by C-terminal phosphorylation. Phosphorylated Smad1/5/8 bind Smad4 and translocate to the nucleus where they regulate expression of target genes, such as *Id* genes. BMP also interacts with members of apico-basal polarity complex as exemplified by early events of neural tube closure (Eom et al., 2011). Loss of Twisted gastrulation gene, encoding a BMP modulator, causes craniofacial defects and affects foregut endoderm and reduced expression of *Hhex*, a transcription factor required for early thyroid development (Petryk et al., 2004). Interestingly, reports on ES cell differentiation have shown that modulation of BMP signalling is critical for efficient lineage specification of Nkx2.1 endodermal progenitors (Green et al., 2011; Longmire et al., 2012;

Kurmann et al., 2015). Since Smads often function redundantly, we studied the role of BMP signalling in the thyroid gland by combined genetic inactivation of Smad1 and Smad5. We found that Smad1/5^{dKO} mice have retarded growth, suffer from hypothyroidism and display a major perturbation in follicle development. Defective folliculogenesis, highly reminiscent of that observed in Vegfa^{KO} mice, was associated with impaired assembly of basement membrane proteins and could be rescued by laminin-rich conditioned medium. Our results indicate that epithelial BMP-Smad1/5 signaling and endothelial cells of the thyroid promote folliculogenesis via assembly of the basement membrane.

Results

Active BMP signaling in thyrocyte progenitors during thyroid development

We first analyzed BMP signaling in thyroid development at the time of follicle formation (from E14.5 to E18.5). Most BMP ligands were expressed in the developing thyroid, and among these, *Bmp2*, *-4*, *-5* and *-7* were the most abundant (Fig. 1A). BMP type I and type II receptors, intracellular *Smad1, -5* and *-8* as well as the common mediator *Smad4*, were also well-expressed (Fig. 1A). Measurement of the absolute copy number of Smad1/5/8 in E14.5 thyroid glands (Fig. 1B) showed that *Smad8* mRNA is approximately four times less abundant than *Smad1* and *Smad5*.

We next assessed whether BMP signaling was active during thyroid development. We first recorded *in vivo* BMP signaling activity in the thyroid region using a transgenic line expressing Green Fluorescent Protein (GFP) under the control of BMP-Responsive Elements (Monteiro et al., 2008). At E14.5, GFP expression was not detected in E-cadherin^{+} thyroid epithelial cells, but was found in the parathyroid and in PECAM^{+} endothelial cells that form blood vessels running along and in between thyroid epithelial cell masses (Fig. 1C). One day later, GFP was detected in some thyroid epithelial cells, and by E16.5 in almost all of the E-cadherin^{+}/thyroglobulin^{+} cells (Fig. 1C). Conversely, GFP colocalization with PECAM was weak at that stage. We further monitored phosphorylation of Smad1/5 by whole-mount analysis of microdissected thyroid lobes (Fig. 1D). In untreated thyroid lobes, we could only detect pSmad1/5 at E15.5, in some E-cadherin^{+} and E-cadherin^{-} cells. However, incubation of E14.5 and E15.5 thyroid lobes in BMP4 induced Smad1/5 phosphorylation and nuclear translocation in epithelial cells (Fig. 1D). This indicated that thyroid epithelial cells are responsive to BMP signaling as early as E14.5 and that signaling is turned on in developing thyroid between E14.5 and E15.5, i.e. at the start and during follicle development.

Smad1/5^{dKO} mice display growth retardation, abnormal follicles and hypothyroidism

To determine the role of BMP signaling in the thyroid, we deleted the most abundant Smads, Smad1 and Smad5, in the thyroid by crossing mice bearing conditional alleles of Smad1 (Smad1$^{fl/fl}$) and Smad5 (Smad5$^{fl/fl}$) with Pax8-Cre mice (Bouchard et al., 2004). Single Smad1^{KO} and Smad5^{K0}, as well as double Smad1/5^{dKO} mice, were viable and born at normal Mendelian ratios. Only Smad1/5^{dKO} displayed smaller body size and significantly reduced body weight at 10 weeks (Fig. 2A). Histological analysis of control thyroids at 10 weeks

showed a collection of large follicles composed of a monolayer of epithelial cells delineating a round lumen (Fig. 2Ba). Single Smad1^{KO} and Smad5^{KO} looked comparable to the control thyroid, although follicles in Smad5^{KO} were somewhat smaller (Fig. 2Bb, Bc). In marked contrast, the thyroid structure of Smad1/5^{dKO} was completely disorganized with much fewer, irregular follicles delineated by taller thyrocytes (Fig. 2Bd). This was accompanied with adipogenesis in Smad1/5^{dKO}, which occurred also to a lesser extent in Smad1^{KO} (data not shown). To evaluate thyroid function, we immunostained sections for iodinated thyroglobulin (Tg). This led to homogeneous staining filling the colloid of all follicles of control and single KO thyroids (Fig. 2Be-g). In Smad1/5^{dKO}, iodinated Tg was limited to a peripheral rim, suggesting colloid depletion due to high turnover rate (Fig. 2Bh). These data suggested that although some thyroid differentiation can occur in Smad1/5^{dKO}, functionality was dramatically affected. Because Smad1/5^{dKO} displayed growth-retardation and histological alterations of the thyroid glands, we next analyzed their thyroid hormonal status at 10 weeks. Plasma T_3 and T_4 concentrations were decreased by five-fold in Smad1/5^{dKO} (Fig. 2C), and accordingly, TSH concentrations were dramatically increased up to 20,000 fold (Fig. 2C). Thus, this major feedback response was insufficient to maintain plasma T_3 and T_4 concentrations (Fig. 2C), demonstrating thyroid unresponsiveness. Taken together, these data indicated that Smad1 and Smad5 are redundantly required for thyroid follicle formation and function.

Smad1/5 are efficiently inactivated in thyrocyte progenitors

The severe follicular alterations and major hypothyroidism of adult Smad1/5^{dKO} mice suggested that follicle formation and/or differentiation might be affected in embryonic thyroid. We first verified Cre-mediated Smad1 and Smad5 recombination by measuring the abundance of *Smad1/5/8* mRNA during early stages of embryonic thyroid development (Fig. 3A). As compared to controls, Smad1/5^{dKO} thyroid showed a 50% reduction in the abundance of *Smad1* and *Smad5* mRNA as early as E14.5, and this reduction persisted until the end of gestation (Fig. 3A). *Smad8* expression, used as a control Smad, was not affected at E14.5 and E16.5. Surprisingly, its level was significantly decreased at E18.5, suggesting positive regulation by BMP-Smad1/5 signaling during thyroid development. Based on epithelial-specific Pax8-Cre expression, we hypothesized that the 50% global reduction in Smad1/5 reflected loss of expression in the developing thyrocytes but persistent expression in other cell types. Further, treating cultured thyroid lobes with BMP4 revealed phosphorylation of Smad1 and Smad5 in control but not in a vast majority of Smad1/5^{dKO} epithelial cells (Fig. 3B).

These data indicated that Smad1/5 were successfully inactivated in thyroid epithelial cells and suggest that the remaining 50% expression in the thyroid can be attributed to Smad1/5 presence in other cell types where the Cre is not induced.

Smad1/5 inactivation impairs thyroid folliculogenesis

Follicle formation from an original mass of non-polarized epithelial cells involves a complex morphogenetic process starting around E14.5. Careful analysis of thyroid gland development reveals progressive fragmentation of the epithelial mass, organization of the epithelial cells in independent spherical structures or rosettes, acquisition of apico-basal polarity and finally lumen expansion (Fagman et al., 2006; Hick et al., 2013). To test when BMP signaling impacts on follicle formation, we analyzed thyroid development in control and Smad1/5^{dKO} mouse embryos from E14.5 to E18.5 (Fig. 3C, E). In controls, dotty immunofluoresccnt labeling for the apical marker, ezrin, first became apparent in the thyroid mass at E14.5, just underneath or fused with the membrane of epithelial progenitors (Fig. 3Ca). We interprete these dots as ezrin-coated vesicles en route to predefined plasma membrane domains, in order to initiate apical pole formation. We frequently observed in sections two such vesicles closely apposed, face to face, next to the plasma membrane of adjacent cells (arrows in Fig. 3C and E). At this stage, the basal marker laminin was only found between thyroid peripheral cells and the stroma (Fig. 3Ea). By E16.5, coordinated fusion of vesicles from several epithelial cells, initiated creation of small lumina. Thyrocyte progenitors organized in microfollicles progressively assembled a laminin-rich basement membrane, appearing as a dense meshwork, which fragmented the mass (Fig. 3Cb, Eb). By the end of gestation, most follicular structures were individualized, i.e. each completely surrounded by laminin (basal pole) and enclosing an expanded lumen circumscribed by ezrin^{+} (apical pole) (Fig. 3Cc, Ec). In the absence of Smad1 and Smad5, the thyroid mass at E14.5 was delineated by a single laminin shell and thyroid epithelial cells contained small dots of ezrin, as in WT controls (Fig. 3Cd, Ed). By E16.5, fusion of ezrin^{+} vesicles with the membrane also occurred, but lumina of microfollicles were much smaller than in WT (Fig. 3Ce, Ee). In addition, the percentage of epithelial cells showing ezrin^{+} membrane revealed a two-fold decrease (83.9± 13.8 % *vs* 35.5 ± 11.7%; Fig. 3F). Fragmentation of the thyroid mass of Smad1/5^{dKO} was also impaired: a large fraction of epithelial cells remained associated in large clusters so that their contact with basement membrane (pan-laminin) was reduced by about half (92.2 ± 7.7 % *vs* 56.7 ± 9.5 %; Fig. 3F). By E18.5, the difference between control and Smad1/5^{dKO} was even more evident. Most epithelial cells remained associated, microfollicles were composed of a reduced number of

cells, only partially delineated by laminin and their lumen did not appreciably expand (Fig. 3Cf, Ef, D). Quantification of sectioned lumen size revealed a four-fold difference in Smad1/5^{dKO} as compared to control (33.9 ± 2.9 μm^2 *vs* 137.1 ± 11.2 μm^2), thus an eight-fold difference in volume. However, the global thyroid size, the thyrocytes proliferation rate and the number of open ezrin$^+$ structures were not affected by Smad1/5 inactivation (data not shown). Altogether, these results indicated that BMP signaling is essential for epithelial reorganization of the thyroid progenitor mass into follicles with large lumina.

Despite the reduced number of ezrin$^+$ epithelial cells and the smaller lumina, we noticed that, when present, ezrin was correctly localized to the apical pole in Smad1/5^{dKO}. This suggested that apical polarity was preserved in these cells. To further test this interpretation, we analyzed control and Smad1/5^{dKO} thyroid for Par3, a key component of the apical polarization machinery, and F-actin for cytoskeleton organization, and found no obvious difference between controls and Smad1/5^{dKO} (Fig. S1A). Furthermore, transmission electron microscopy revealed that epithelial cells involved in immature microfollicles in Smad1/5^{dKO} still developed tight junctions and microvilli projecting into the lumen space, as in control follicles (Fig. S1B). However, intracellular microvilli inclusion bodies were observed in Smad1/5^{dKO}, suggesting defective apical delivery of intracellular vesicles (Fig. S1B, inset). Altogether, these data indicated that BMP-Smad signaling controls folliculogenesis downstream of the initial apical specification but upstream of basement membrane assembly, epithelial reorganization and lumen expansion.

Smad1/5 signaling in thyrocytes stimulates *Vegfa* expression and affects gene expression in neighboring endothelial cells

Previous work from our group has shown that endothelial cell recruitment into the developing thyroid is required for follicle formation. The folliculogenic effect of endothelial cells was contact-independent and could be mimicked with medium conditioned by endothelial cells (Hick et al., 2013). We thus tested whether defective folliculogenesis in Smad1/5^{dKO} could be due to lack of either endothelial cells, or a signal derived therefrom. We identified endothelial cells by immunofluorescence for PECAM, a cell adhesion molecule specifically expressed by endothelial cells, in control and Smad1/5^{dKO} thyroids from E14.5 to E18.5 (Fig. 4A). In control and Smad1/5^{dKO} thyroids, the abundance and localization of blood vessels were unaffected at the three stages analyzed (Fig. 4A). Quantification of endothelial sectioned

surface and epithelial-to-endothelial sectioned surface ratio did not reveal any significant difference.

To evaluate endothelial cell differentiation in Smad1/5^{dKO}, we measured the expression of selected endothelial-specific genes. We found that expression of *vascular endothelial cadherin-1* (*Cdh5*) and *-2* (*Pcdh12*) as well as of *Tie1* was significantly reduced at E16.5 (Fig. 4B), but expression of *Vegfr2, Pecam1* and *endothelial cell-specific molecule 1* (*Esm1*) was normal. *Vegfa* controls endothelial cell development and BMP-Smad1/5 signaling is known to control *Vegfa* expression in several cell types (Bai et al., 2013; Deckers et al., 2002; Shao et al., 2009; Shimizu et al., 2012). Therefore we measured *Vegfa* in developing Smad1/5^{dKO} thyroids and found that it was reduced starting at E14.5; this reduction reached statistical significance starting at E16.5 (Fig. 4C). We thus directly analyzed the effect of BMP addition on *Vegfa* expression in microdissected thyroid lobes at E14.5 and in the thyroid follicular cell line, FRTL-5. Treatment of thyroid lobes with the specific BMP inhibitor, DMH1(Hao et al., 2010), led to a reduction in *Vegfa* expression and of the BMP-Smad1/5 signaling target gene *Id2* (Fig. 4D). Incubation of wild-type thyroid lobes with BMP ligands induced *Id2*, but did not modify the already high *Vegfa* expression (Hick et al., 2013). To circumvent BMP accessibility issue we incubated the thyroid cell line FRTL-5 with a combination of the most abundant BMP ligands in the thyroid (BMP2, -4, -5 and -7) and noticed a dose-dependent stimulation of the expression of *Vegfa* and *Id2* (Fig. 4E). These results indicated that epithelial Smad1/5 signaling regulates *Vegfa* and endothelial gene expression.

Production of the basement membrane proteins laminin and type IV collagen, is decreased in Smad1/5^{dKO} and Vegfa^{KO} thyroid glands

We next turned to the identification of the follicle promoting factor(s). Knowing that thyrocytes and endothelial cells form their own continuous basement membrane, that extracellular matrix components promote epithelial cell organization, and that contact with laminin was partly impaired in Smad1/5^{dKO}, we postulated that the basement membrane could stimulate folliculogenesis. To test this hypothesis, we first looked for a possible defect of *laminin* and *type IV collagen* expression in Smad1/5^{dKO} and Vegfa^{KO} (Fig. S2). Laminins are a family of 5 α, 3 β and 3 γ chains forming $\alpha\beta\gamma$ heterotrimers that span the basement membrane. Collagen type IV family has 6 α chains forming trimers interconnected with the laminin network.

In Smad1/5^{dKO}, expression of *laminins α2, α3, β1* and *β3* chains was significantly albeit transiently reduced (Fig. S2A, B). Expression of *laminin α3* and *α4* was significantly reduced in Vegfa^{KO} (Fig. S2C). Of note, laminin α4 displays an endothelial-specific pattern in E16.5 embryos (Matrixome). A similar analysis revealed a reduction of most of *type IV collagen* genes in Smad1/5^{dKO} (Fig. S2D). There was an important and sustained reduction in *collagen α3-6 (IV)* chains. *Collagen α1(IV)* and *α2(IV)* were modestly reduced or delayed. In Vegfa^{KO}, expression of *collagen α1(IV)* and *α2(IV)* was significantly reduced (Fig. S2E); both genes were also reported as endothelial-specific (Matrixome). In conclusion, gene expression analysis revealed decreased expression of several basement membrane proteins in Smad1/5^{dKO} and Vegfa^{KO}.

We next examined by immunofluorescence whether decreased gene expression resulted in impaired basement membrane assembly. In line with the gene expression analysis, collagen type IV signals were severely affected in both KO (Fig 5Ab, d). Pan-laminin signals were also reduced in Smad1/5^{dKO} and only modestly in Vegfa^{KO} (Fig 5Af, h). Taken together, these data indicated that expression and/or deposition of basement membrane proteins depends on endothelial cells and Smad1/5 signaling in thyrocytes, and suggested an essential role for basement membrane assembly in folliculogenesis.

Epithelial laminin production is affected in Smad1/5^{dKO}

Mature angio-follicular units are characterized by close proximity between endothelial and epithelial cells. To determine the respective contribution of epithelial and endothelial cells to basement membrane proteins synthesis, we analyzed the expression of laminin and collagen type IV genes in FACS-sorted epithelial populations (Fig. S3). Epithelial thyrocyte progenitors were selected based on YFP expression after Pax8-cre mediated recombination of ROSA-STOP-YFP locus. This population was compared to YFP$^-$ cells, which thus included C-cells, endothelial and mesenchymal cells but also non-recombined thyrocyte progenitors. *Yfp* mRNA was only found in the YFP$^+$ cells. *Pax8* and the epithelial marker *E-cadherin* showed a two-fold enrichment in this population, while *Vegfr2* was enriched four-fold in the YFP$^-$ population, as expected (Fig. S3A). mRNAs for all collagens type IV as well as *laminins α3, β1-3* and *γ1-2* were equally distributed in YFP$^+$ and YFP$^-$ thyroid cells. In contrast, *laminin α1* and *α5* chains were enriched in the YFP$^+$ epithelial population while *laminin α2* and *α4* chains showed the strongest expression in YFP$^-$ population (Fig. S3B).

Since laminins α1 and α5 were enriched in the epithelial population, we studied their expression by immunofluorescence using isoform-specific antibodies. In control thyroid glands, epithelial follicular structures were surrounded by almost continuous laminin α1 and α5 signal. In Smad1/5^{dKO} thyroids, laminin α1 signal was severely reduced (Fig. 5B), supporting the RT-qPCR analysis (Fig. S2A). Laminin α5 signal was comparable to controls, although the pattern was affected due to epithelial organization defect (Fig. 5C). These data confirmed that the key basement membrane proteins, laminin and collagen type IV, are produced by both epithelial and endothelial components of the angio-follicular units, and indicated that Smad1/5^{dKO} epithelial cells have impaired ability to produce and assemble laminin α1-containing heterotrimers.

Medium conditioned by endothelial cells contains folliculogenic factor(s) and rescues follicle formation defect of Smad1/5^{dKO} and Vegfa^{KO}

To investigate the mechanism of follicle formation, we resorted to an *ex vivo* culture system of thyroid lobes. We had previously reported that pharmacological ablation of endothelial cells in E12.5 thyroid explants prevented folliculogenesis; conversely, addition of CM by embryonic endothelial progenitor cells (eEPC), herein referred to as eEPC-CM, was able to rescue - and even overstimulate follicle formation (Hick et al., 2013). Using an improved thyroid lobe culture system (Delmarcelle et al., 2014), we here report that addition of eEPC-CM to non-ablated wild-type thyroid lobes promotes follicle development by up to six-fold after 3 days of culture (Fig. 6A, C). This medium thus contains folliculogenic factor(s). We thus addressed whether such eEPC-CM could rescue defective folliculogenesis of Smad1/5^{dKO} and Vegfa^{KO}. We first verified that E14.5 Smad1/5^{dKO} thyroid lobes reproduce impaired follicle formation upon *ex vivo* culture: only very small ezrin^{+} structures could be observed after 3 days (Fig. 6B). Importantly, eEPC-CM significantly induced follicle formation in Smad1/5^{dKO} thyroid lobes (Fig. 6B, C), and the same was found for Vegfa^{KO} (Fig. S4). The similar rescue of immature microfollicle development of Smad1/5^{dKO} and Vegfa^{KO} thyroid glands-by folliculogenic factor(s) of eEPC-CM suggested that these factor(s) act downstream of epithelial Smad1/5 signaling and of endothelial cells.

Laminins deposited and assembled around thyroid epithelial cells, promote folliculogenesis.

Among potential folliculogenic factors, we examined whether eEPC expressed and released basement membrane proteins into their conditioned medium. We first determined the expression profile of laminin subunit and collagen type IV genes in eEPC. We found that eEPC express very high levels of *laminin α1, β1* and *γ1* mRNAs, which almost reached the level of *β-actin* housekeeping gene (Fig. 7A). Among collagen type IV genes, *α6* showed the highest level of expression, albeit approximately 1000X lower than *laminin β1*. We next verified that eEPC can secrete laminins into the CM, in particular laminin-111 (heterotrimer of α1, β1 and γ1), by silver staining, western blotting and mass spectrometry. Silver staining after SDS-PAGE of CM revealed a well-defined band migrating at a similar M_r as purified laminin-111 (Fig. 7B). Western blotting with laminin α1 specific antibody identified this subunit (Fig. 7B). Mass spectrometry further easily detected laminin α1, laminin β1 and laminin γ1 peptides in the CM (Table S1). Finally, we asked whether laminin-111 from eEPC-CM was deposited on cultured E14.5 thyroid lobes. Immunofluorescence for laminin α1 revealed a much stronger signal after 1 day of incubation with the CM, as compared to untreated explants. This signal further increased after 2 and 3 days of culture and became organized around peripheral epithelial structures (Fig. 7C). These data indicated that laminin-111, which is expressed and secreted by eEPC in the medium, can be assembled around epithelial structures of thyroid lobes.

To confirm that laminin-111 acts as a folliculogenic factor, we inhibited its production in eEPC. Silencing laminin α1 in eEPC by shRNA yielded CM abrogated its folliculogenic activity on thyroid lobes (Fig. 7D, E), while preventing the accrued deposition of laminin α1 in thyroid lobes (Fig. 7E). Similar results were obtained upon laminin β1 and laminin γ1 silencing (data not shown). These data indicated that laminin-111 in eEPC-CM is a key actor of thyroid folliculogenesis.

Discussion

In this paper, we examined if and how BMP/Smad signalling is required for thyroid follicle formation. We found that BMP signalling was activated in thyroid epithelial cells during folliculogenesis. Inactivation of Smad1/5 in thyroid epithelium caused major alterations of follicular structures, hypothyroidism and growth retardation but no loss of viability. Defective follicular development was associated with impaired basement membrane assembly, highly reminiscent of the folliculogenesis defect of $Vegfa^{KO}$ embryos in which endothelial cells are however absent. Follicle formation defects in $Smad1/5^{dKO}$ and $Vegfa^{KO}$ could be rescued with laminin-rich conditioned medium. Taken together, our findings support a model in which thyroid follicle formation depends on basement membrane assembly, a process controlled by epithelial Smad1/5 signaling and endothelial cells.

Ten-week-old $Smad1/5^{dKO}$ were smaller and had a reduced body weight as compared to control littermates. Failure to grow is readily explained by the very low levels of thyroid hormones, T_3 and T_4, and extremely high TSH values demonstrated non-compensated hypothyroidism. Thyroid unresponsiveness despite huge TSH values is well known in KOs mice for the TSH receptor, Nkx2.1, Foxe1 and Pax8 (De Felice and Di Lauro, 2004). Although, $Smad1/5^{dKO}$ thyroid lobes at birth had a normal size, the functional impairment of adult thyroid probably results from the embryonic folliculogenesis defects. However, we cannot exclude a role for BMP signaling in postnatal thyroid homeostasis.

Our laboratory has evidenced that follicle formation occurs by reorganization of the thyroid primordium epithelial cell mass into polarized monolayers surrounding a central lumen i.e. comparable to the cord hollowing model of *de novo* lumen formation (Andrew and Ewald, 2010) and the process of apico-basal polarization with lumen formation as observed in MDCK cells when cultured in a three-dimensional matrigel. In this 3D culture system, fusion of vesicles to the Apical Membrane Initiation Site (AMIS) allows apical lumen opening and cyst formation (Bryant et al., 2010). In the thyroid, we also observed pre-apical intracellular vesicles ($ezrin^+$) and their coordinate exocytosis to generate apical lumen. Immature microfollicles can then expand or enlarge, while segregating from adjacent ones and becoming vascularized by invading endothelial cells. In $Smad1/5^{dKO}$, despite formation of $ezrin^+$ vesicles in some cells and endothelial invasion, exocytosis of vesicles with membranes and lumen expansion were clearly impaired, as were fragmentation of the mass, leading to individualization of microfollicles.

The occurrence of immature microfollicles in Smad1/5^{dKO} thyroid suggests that the basal machineries for apical polarization and for creation of secluded lumina are preserved. However, this does not mean that these machineries are quantitatively fully operative. Indeed, we found that much fewer epithelial cells (i) participate in microfollicle formation (Fig. 3D); (ii) develop an ezrin^{+} apical pole (Fig. 3F); and (iii) assemble a basal laminin^{+} pole (Fig. 3F). Altogether, these data indicate that although some epithelial cells in Smad1/5^{dKO} thyroid engage into polarization and formation of a secluded lumen, much fewer participate in this concerted process when BMP signalling is inactivated. These observations suggest either that BMP signalling is not required for apical polarization, or that the genetic inactivation using the Cre recombinase is not 100% effective in all the Pax8^{+} cells at the same time and for the four Smad alleles. Progression of immature microfollicles into larger structures, clearly affected in Smad1/5^{dKO}, cannot be explained by impaired epithelial proliferation (normal rate in Smad1/5^{dKO}). Conceivably, impaired follicle enlargment could be related to defective differentiation, thus lower accumulation of thyroglobulin that could force expansion of the colloid lumen. However, Vegfa^{KO}, which also displays immature microfollicles, express almost normal thyroglobulin level (90% of wild-type; Hick et al., 2013). This observation argues that thyroglobulin accumulation is not sufficient for lumen expansion. Comparison of Smad1/5^{dKO} and Vegfa^{KO} rather suggests that lumen enlargement depends on correct apico-basal polarization. Indeed, as compared to aged-matched control littermates, we found in both Smad1/5^{dKO} and Vegfa^{KO} (i) reduced basement membrane deposition; and (ii) persistence of intracellular ezrin^{+} vesicles, suggesting a relation between basement membrane-triggered polarization and impaired fusion with the apical membrane (Supplementary Figure 1B and Fig. 3C and E, arrows).

Impaired follicle formation observed in the absence of Smad1 and Smad5 is reminiscent of the defect observed in the absence of endothelial cells, upon *Vegfa* inactivation in thyroid epithelium (Hick et al., 2013). Although endothelial cell density in epithelial-specific Smad1/5^{dKO} was comparable to that of control thyroid glands, expression of endothelial cell identity markers (*Cdh5*, *Pcdh12* and *Tie1)* and endothelial-enriched basement membrane proteins (*type IV collagen α1*, *α2* and *laminin α3*) was impaired, consistent with ongoing reciprocal paracrine communications between epithelial and endothelial cells (Hick et al., 2013). In this report, we further found that BMP/Smad signaling in thyroid epithelial cells controls the expression of *Vegfa*, in agreement with reports in other cell types (Bai et al., 2013; Deckers et al., 2002; Shao et al., 2009; Shimizu et al., 2012). Of note, this regulation in

zebrafish could be either positive (for Smad1) or negative (for Smad5)(He and Chen, 2005). Our findings in developing thyroid suggest instead that BMPs could control endothelial gene expression program indirectly, i.e. by regulating *Vegfa* expression. Changes of gene expression in endothelial cells could in turn impact on follicle formation. Several studies have emphasized the critical role played by endothelial cells via angiocrine factors in the regulation of organ morphogenesis (Ramasamy et al., 2015). Integrating available knowledge supports a reciprocal paracrine communication in which thyrocyte progenitors, under the influence of BMP, participate in the recruitment and maturation of thyroid endothelial cells, via VEGFa. In turn, endothelial cells invasion and maturation in the thyroid mass would create a microenvironment permissive for folliculogenesis.

The importance of the extracellular environment for cell polarization in tissue culture experiments has long been recognized (Wang et al., 1990a; Wang et al., 1990b). Culture of the MDCK epithelial cells in collagen-rich gel or matrigel triggers production of laminin and assembly of a basement membrane, which in turn promotes cystic structures (Bryant et al., 2010), a process which can be directly compared to the formation of thyroid follicles. In addition, ES cells, when forced to transiently co-express Pax8 and Nkx2.1 transcription factors, differentiate into thyrocytes progenitors that can form functional follicles if further cultured in matrigel (Antonica et al., 2012; Ma et al., 2015). These two convergent *in vitro* studies emphasize the critical role of basement membrane and extracellular matrix proteins for the development of a three-dimensional, cyst-like, or follicular structure.

In vivo, we observed reduced expression of laminin α1 and collagen type IV in Smad1/5^{dKO}. Few reports have suggested a direct role for BMP signaling in basement membrane synthesis and deposition. During *ductus arteriosus* closure, BMP-9 and -10 are required to stimulate endothelial cell differentiation and extracellular matrix deposition (Levet et al., 2015). In kidney mesangial cells, Smad1 directly controls the expression of collagen type IV-α1 and -α2, which leads to glomerular basement membrane thickening (Abe et al., 2004; Matsubara et al., 2015). Thus, cumulative evidence indicates that BMP/Smad signalling can regulate tissue morphogenesis by controlling the expression and/or deposition of extracellular matrix proteins.

Analysis of basement membrane proteins in Vegfa^{KO} also revealed decreased type IV collagen signal (Fig. 5A), most probably due to the absence of endothelial cells (Hick et al., 2013). In addition, we found impaired epithelial laminin α1 assembly in Vegfa^{KO} (data not

shown). This suggests that endothelial cell invasion into the epithelial mass, by disrupting multidirectional epithelial cell-cell contacts and inducing interstitial matrix deposition that individualize cell cords then microfollicles, would indirectly stimulate epithelial basement membrane assembly, like in MDCK cells grown in matrigel.

Laminin deposition is the primary event of basement membrane formation, and induces the secondary assembly of type IV collagen meshwork (Morrissey and Sherwood, 2015; Poschl et al., 2004). In turn, the collagen IV meshwork is essential for integrity, stability and functionality of the basement membrane (Poschl et al., 2004; Yurchenco, 2011). We thus propose that addition of exogenous, eEPC-derived, laminin-111 was sufficient to stimulate the organization of epithelial cells in follicles in control thyroid lobes, and to rescue follicle formation defects in Smad1/5^{dKO} and Vegfa^{KO}, by promoting assembly of endogenous laminin and type IV collagens scaffolds. Rescue of folliculogenesis in Smad1/5^{dKO} and Vegfa^{KO} thus indicates that basement membrane assembly is a critical step in folliculogenesis, downstream of epithelial BMP signaling and of endothelial cell invasion.

In conclusion, we propose a model placing epithelial basement membrane assembly in developing thyroid gland as a critical signal to orient epithelial cell polarization and promote their organization into follicles. First, epithelial cells from the thyroid primordium produce VEGFa; at this step, epithelial BMP/Smad signaling participates in Vegfa gene expression. Second, upon VEGFa-dependent endothelial cell recruitment and invasion into the thyroid epithelial cell mass, multidirectional epithelial cell-cell contacts are disrupted while lateral contacts are preserved. This triggers, together with continued BMP-Smad signalling, epithelial production and deposition of their own basement membrane proteins. Finally, epithelial basement membrane assembly orient the epithelial cells, promote apical delivery of ezrin^{+} vesicles and individualization of follicles.

Materials and Methods

Animals

Smad1/5-floxed, Vegfa-floxed, Pax8-Cre and BRE-GFP mice were obtained from A. Zwijsen and E.J. Robertson (Arnold et al., 2006; Umans et al., 2003), N. Ferrara (Genentech) (Gerber et al., 1999), M. Busslinger (Bouchard et al., 2004) and S.M. Chuva de Sousa Lopes (Monteiro et al., 2008), respectively. All other mice were of the CD1 strain. Mice were raised and treated according to the guidelines of laboratory animal care of the University Animal Welfare Committee, UCL.

Dissection and culture of thyroid explants

Thyroid lobes were microdissected from E14.5 mouse embryos and processed as described (Delmarcelle et al., 2014). DMH1 (Sigma-Aldrich) was dissolved in DMSO and used at 3 or 10 µM. Recombinant mouse BMP4 (R&D Systems) was reconstituted at 100 µg/ml in 4 mM HCl containing 0.1% BSA and added at 20 ng/ml in the culture medium. Control explants were exposed to the same concentration of vehicle as the test samples. Thyroid lobes were maintained in culture during 3 or 4 days, and processed for RNA extraction and immunolabelling as described (Delmarcelle et al., 2014).

Histology, immunolabelling and morphometric analyses

Thyroids were microdissected and fixed for 1 hour with 4% formaldehyde in PBS and processed for paraffin embedding. 8 µm-thick sections were stained with hematoxylin and eosin staining. Immunofluorescence on sections thyroid gland sections from embryos or explants was performed as described previously (Pierreux et al., 2006) . Antibodies and dilutions are shown in Table S2. Nuclei were counterstained with Hoechst (Sigma) in PBS during incubation with secondary antibody. For immunoperoxidase, the envision system (Dako) was used. Whole histological sections were recorded with Mirax Scan (Zeiss). Fluorescence on sections was observed with a Zeiss Cell Axiovert 200 inverted fluorescence microscope or with a Zeiss Cell Observer Spinning Disk (COSD). For quantification of follicles, at least 18 sections in 4 independent explants were counted. Endothelial and epithelial surface was quantified using the Axiovision 4.8.2 software (Zeiss). Briefly, images were prepared as binary mask, filled and the surface area was calculated on 6 images/sections spanning 360 µm of 3 controls and 3 Smad1/5^{dKO} thyroids. The epithelial: endothelial surface ratio was finally calculated.

T_3, T_4 and TSH level measurements

T_3 and T_4 concentrations were measured by coated-tube RIA (Siemens Medical Solution Diagnostics). Plasma Thyroid-stimulating hormone (TSH) concentrations were measured using a sensitive, heterologous, disequilibrium double-antibody precipitation RIA as described previously (Pohlenz et al., 1999). Hormone levels were measured in 16 female and 15 male mice.

RNA extraction and Real-time RT-PCR

Total RNA was extracted from microdissected thyroid lobes, cultured explants or FRTL-5 cells using Trizol reagent and phenol/chloroform extraction (Delmarcelle et al., 2014). RNA (0.5–1 µg) was reverse-transcribed with random hexamers using Moloney Murine Leukemia Virus reverse transcriptase (Invitrogen). Real-time quantitative PCR was performed by using KAPA^{TM} SYBR® Fast qPCR kit (Sopachem). Primers sequences are described in Table S3. *β-actin* and *RPL27* were used as reference genes and relative changes in target gene/reference gene mRNA ratio were determined by transformation of threshold cycles to absolute mRNA numbers (Dupasquier et al., 2014) or using the ΔΔct method.

Endothelial progenitor cells (EPCs) conditioned medium (CM)

Previously established mouse embryonic EPCs (Hatzopoulos et al., 1998; Kupatt et al., 2005) were used for no more than 6 months after being thawed, as described (Sbaa et al., 2006). The preparation of CM was adapted from (Hick et al., 2013). Briefly, 90% confluent cells were incubated for 24 h in M199 medium without serum (6 ml for a 7.8 cm^2 dish). Supernatant was first centrifuged at 1900 *g* for 5 min to remove floating cells or large debris, then at 17000 *g* for 20 min and finally concentrated 10-x by centrifugation at 1900 *g* for 5 min in Amicon Ultra 50K units. 10-x concentrated medium was supplemented with 10% FCS before use. Mass spectrometry was performed as described (Cho et al., 2014).

Cell culture

Fisher rat thyroid follicular FRTL-5 cells (Sigma) were cultured in Coon's modified F12 medium as previously described (Craps et al., 2015) and were used within 6 months of purchase. Cells were grown in 12-well tissue culture dishes for 24 h before treatment with BMP ligands. Recombinant mouse BMP 2, -4, -5 and -7 (R&D Systems) were reconstituted in 4 mM HCl containing 0.1% BSA at 100 – 150 µg/ml and used as a mix of 25 ng/ml

(BMP2), 5 ng/ml (BMP4), 150 ng/ml (BMP5) and 75 ng/ml (BMP7). After 8 h, cells were lysed in Trizol reagent and RNA was extracted.

Lentiviral infection

Lentiviral constructs driving expression of shRNA against laminin α1 were generated as described previously (Gerin et al., 2010). Briefly, the pGIPZ lentiviral vectors containing a shRNA against laminin α1, α5, β1 and γ1 or the pGIPZ empty vector (Openbiosystems) were transfected in HEK293T for lentiviral production. Packaging was performed using a second generation plasmid system (psPAX2 and pMD2.G; Addgene plasmids 12,259 and 12,260, respectively) by transient transfection with the calcium phosphate co-precipitation method. We used 8.4 µg of lentiviral vectors, 8.4 µg of psPAX2 and 4.2 µg of pMD2.G per 6-cm tissue culture dish. After 24 h of transfection, EPC cells were infected with filtrated lentiviral particles and 4mg/ml of Polybrene (Sigma). Infected cells were selected for 4 days with 2 µg/ml of puromycin (Merck). CM was prepared as above.

Western blotting

Western blotting was performed as described (Cominelli et al., 2014). Briefly, cells were lysed in RIPA buffer and protein concentration was measured using bicinchoninic acid. 30 µg of cell protein extract or a corresponding volume of 10-x CM was loaded with 2% SDS and 10 mM DTT sample buffer on 5% polyacrylamide gels (4% stacking gel), resolved by SDS-PAGE and transferred onto PVDF membrane (Polyscreen ® PVDF Transfer Membrane, Perkin Elmer). Blots were blocked and incubated overnight at 4°C with the primary antibody (rabbit anti-laminin α1, 1/1000, gift from Takako Sasaki; mouse anti-ezrin, 1/1000, Thermo Scientific). After washes and incubation with the appropriate secondary antibody, immunoreactive bands were visualized using chemiluminescence (Supersignal West Femto Maximum sensitivity substrate mixed with Supersignal West Pico chemiluminescent substrate, Thermo Scientific) and acquired using a 4000MM Kodak Image Station (Eastman Kodak Co.). For silver staining, gels are stained using the Silverquest Staining Kit (Invitrogen).

Electron microscopy

Control and Smad1/5^{dKO} thyroid lobes were rinsed with 155 mM NaCl, fixed by 2% (v/v) glutaraldehyde in 0.1 M sodium cacodylate buffer, pH 7.4 for 30 min at 4°C and washed thrice with 50 mM Tris-HCl, pH 6.0 for 10 min. Cells were post-fixed with 1% (w/v) OSO_4-

2%$KFe(CN)_6$ solution (reduced osmium) and stained “en bloc” with 1% uranyl acetate for 2 h and pelleted in 2% agar. Pellets were dehydrated in graded ethanol and embedded in Spurr. Ultrathin (70 nm nominal) sections were obtained with a Reichert ultramicrotome (Reichert), collected on rhodanium 400 mesh grids and contrasted with 3% uranyl acetate followed by lead citrate, each for 10 min. Grids were washed with water, dried, and analysed in a FEI CM12 electron microscope operating at 80 kV.

Statistics

Sample size was defined based on previous expertise. Mann Whitney U test and One-way ANOVA followed by Bonferroni’s multiple comparison tests were performed using Prism software.

Acknowledgements:

We thank T. Sasaki for purified laminin and antibodies, J. Miner for anti-laminin antibodies and Ris-Stalpers for iodo-thyroglobulin antibody. We also thank J-F. Collet and D. Vertommen for biochemical assistance, J. Craps for the FRTL-5 cell line, S. Costagliola and S. Ascenzo for discussions and S. Cordi for technical advices. This work was supported in part by grants from F.R.S.-FNRS, ARC, Fondation Roi Baudouin, Interuniversity Attraction Poles-Phase VII [IUAP/PAI P7/14], Belgium and DK15070 from the National Institutes of Health, USA. MV was supported by FSR-UCL, ASD by Télévie, and GB, PH and CEP are Research Associate of the F.R.S.-FNRS.

Author Contributions

MV and ASD designed and performed the experiments and wrote the manuscript. ML, MB, PL, JB, LU, PVDS and SR performed experiments. SCSL provided the BRE mouse line. TS, GB, PH, FL, SR, AZ and PC contributed intellectually and edited the manuscript. CEP conceived the project, contributed experimental and intellectual advice and edited the manuscript.

Conflict of Interest

The authors declare that they have no conflict of interest.

References

Abe, H., Matsubara, T., Iehara, N., Nagai, K., Takahashi, T., Arai, H., Kita, T. and Doi, T. (2004). Type IV collagen is transcriptionally regulated by Smad1 under advanced glycation end product (AGE) stimulation. *J Biol Chem* **279**, 14201-14206.

Andrew, D. J. and Ewald, A. J. (2010). Morphogenesis of epithelial tubes: Insights into tube formation, elongation, and elaboration. *Dev Biol* **341**, 34-55.

Antonica, F., Kasprzyk, D. F., Opitz, R., Iacovino, M., Liao, X. H., Dumitrescu, A. M., Refetoff, S., Peremans, K., Manto, M., Kyba, M., et al. (2012). Generation of functional thyroid from embryonic stem cells. *Nature* **491**, 66-71.

Arnold, S. J., Maretto, S., Islam, A., Bikoff, E. K. and Robertson, E. J. (2006). Dose-dependent Smad1, Smad5 and Smad8 signaling in the early mouse embryo. *Dev Biol* **296**, 104-118.

Bai, Y., Wang, J., Morikawa, Y., Bonilla-Claudio, M., Klysik, E. and Martin, J. F. (2013). Bmp signaling represses Vegfa to promote outflow tract cushion development. *Development* **140**, 3395-3402.

Bouchard, M., Souabni, A. and Busslinger, M. (2004). Tissue-specific expression of cre recombinase from the Pax8 locus. *Genesis* **38**, 105-109.

Bryant, D. M., Datta, A., Rodriguez-Fraticelli, A. E., Peranen, J., Martin-Belmonte, F. and Mostov, K. E. (2010). A molecular network for de novo generation of the apical surface and lumen. *Nat Cell Biol* **12**, 1035-1045.

Cho, S. H., Szewczyk, J., Pesavento, C., Zietek, M., Banzhaf, M., Roszczenko, P., Asmar, A., Laloux, G., Hov, A. K., Leverrier, P., et al. (2014). Detecting envelope stress by monitoring beta-barrel assembly. *Cell* **159**, 1652-1664.

Colin, I. M., Denef, J. F., Lengele, B., Many, M. C. and Gerard, A. C. (2013). Recent insights into the cell biology of thyroid angiofollicular units. *Endocr Rev* **34**, 209-238.

Cominelli, A., Gaide Chevronnay, H. P., Lemoine, P., Courtoy, P. J., Marbaix, E. and Henriet, P. (2014). Matrix metalloproteinase-27 is expressed in CD163+/CD206+ M2 macrophages in the cycling human endometrium and in superficial endometriotic lesions. *Mol Hum Reprod* **20**, 767-775.

Craps, J., Wilvers, C., Joris, V., De Jongh, B., Vanderstraeten, J., Lobysheva, I., Balligand, J. L., Sonveaux, P., Gilon, P., Many, M. C., et al. (2015). Involvement of nitric oxide in iodine deficiency-induced microvascular remodeling in the thyroid gland: role of nitric oxide synthase 3 and ryanodine receptors. *Endocrinology* **156**, 707-720.

De Felice, M. and Di Lauro, R. (2004). Thyroid development and its disorders: genetics and molecular mechanisms. *Endocr Rev* **25**, 722-746.

Deckers, M. M., van Bezooijen, R. L., van der Horst, G., Hoogendam, J., van Der Bent, C., Papapoulos, S. E. and Lowik, C. W. (2002). Bone morphogenetic proteins stimulate angiogenesis through osteoblast-derived vascular endothelial growth factor A. *Endocrinology* **143**, 1545-1553.

Delmarcelle, A. S., Villacorte, M., Hick, A. C. and Pierreux, C. E. (2014). An ex vivo culture system to study thyroid development. *J Vis Exp*.

Dupasquier, S., Delmarcelle, A. S., Marbaix, E., Cosyns, J. P., Courtoy, P. J. and Pierreux, C. E. (2014). Validation of housekeeping gene and impact on normalized gene expression in clear cell renal cell carcinoma: critical reassessment of YBX3/ZONAB/CSDA expression. *BMC Mol Biol* **15**, 9.

Eom, D. S., Amarnath, S., Fogel, J. L. and Agarwala, S. (2011). Bone morphogenetic proteins regulate neural tube closure by interacting with the apicobasal polarity pathway. *Development* **138**, 3179-3188.

Fagman, H., Andersson, L. and Nilsson, M. (2006). The developing mouse thyroid: embryonic vessel contacts and parenchymal growth pattern during specification, budding, migration, and lobulation. *Dev Dyn* **235**, 444-455.

Fagman, H. and Nilsson, M. (2010). Morphogenesis of the thyroid gland. *Mol Cell Endocrinol* **323**, 35-54.

Gerber, H. P., Hillan, K. J., Ryan, A. M., Kowalski, J., Keller, G. A., Rangell, L., Wright, B. D., Radtke, F., Aguet, M. and Ferrara, N. (1999). VEGF is required for growth and survival in neonatal mice. *Development* **126**, 1149-1159.

Gerin, I., Clerbaux, L. A., Haumont, O., Lanthier, N., Das, A. K., Burant, C. F., Leclercq, I. A., MacDougald, O. A. and Bommer, G. T. (2010). Expression of miR-33 from an SREBP2 intron inhibits cholesterol export and fatty acid oxidation. *J Biol Chem* **285**, 33652-33661.

Green, M. D., Chen, A., Nostro, M. C., d'Souza, S. L., Schaniel, C., Lemischka, I. R., Gouon-Evans, V., Keller, G. and Snoeck, H. W. (2011). Generation of anterior foregut endoderm from human embryonic and induced pluripotent stem cells. *Nat Biotechnol* **29**, 267-272.

Hao, J., Ho, J. N., Lewis, J. A., Karim, K. A., Daniels, R. N., Gentry, P. R., Hopkins, C. R., Lindsley, C. W. and Hong, C. C. (2010). In vivo structure-activity relationship study of dorsomorphin analogues identifies selective VEGF and BMP inhibitors. *ACS Chem Biol* **5**, 245-253.

Hatzopoulos, A. K., Folkman, J., Vasile, E., Eiselen, G. K. and Rosenberg, R. D. (1998). Isolation and characterization of endothelial progenitor cells from mouse embryos. *Development* **125**, 1457-1468.

He, C. and Chen, X. (2005). Transcription regulation of the vegf gene by the BMP/Smad pathway in the angioblast of zebrafish embryos. *Biochem Biophys Res Commun* **329**, 324-330.

Hick, A. C., Delmarcelle, A. S., Bouquet, M., Klotz, S., Copetti, T., Forez, C., Van Der Smissen, P., Sonveaux, P., Collet, J. F., Feron, O., et al. (2013). Reciprocal epithelial:endothelial paracrine interactions during thyroid development govern follicular organization and C-cells differentiation. *Dev Biol* **381**, 227-240.

Kupatt, C., Horstkotte, J., Vlastos, G. A., Pfosser, A., Lebherz, C., Semisch, M., Thalgott, M., Buttner, K., Browarzyk, C., Mages, J., et al. (2005). Embryonic endothelial progenitor cells expressing a broad range of proangiogenic and remodeling factors enhance vascularization and tissue recovery in acute and chronic ischemia. *FASEB J* **19**, 1576-1578.

Kurmann, AA., Serra, M., Hawkins, F., Rankin, SA., Mori, M., Astapova, I., Ullas, S., Lin, S., Bilodeau, M., Rossant, J., et al. (2015). Regeneration of thyroid function by transplantation of differentiated pluripotent stem cells. Cell Stem Cell **17**, 1-16.

Lammert, E., Cleaver, O. and Melton, D. (2001). Induction of pancreatic differentiation by signals from blood vessels. *Science* **294**, 564-567.

Lazarus, A., Del-Moral, P. M., Ilovich, O., Mishani, E., Warburton, D. and Keshet, E. (2011). A perfusion-independent role of blood vessels in determining branching stereotypy of lung airways. *Development* **138**, 2359-2368.

Levet, S., Ouarne, M., Ciais, D., Coutton, C., Subileau, M., Mallet, C., Ricard, N., Bidart, M., Debillon, T., Faravelli, F., et al. (2015). BMP9 and BMP10 are necessary for proper closure of the ductus arteriosus. *Proc Natl Acad Sci U S A* **112**, E3207-3215.

Longmire, T. A., Ikonomou, L., Hawkins, F., Christodoulou, C., Cao, Y., Jean, J. C., Kwok, L. W., Mou, H., Rajagopal, J., Shen, S. S., et al. (2012). Efficient derivation of purified lung and thyroid progenitors from embryonic stem cells. *Cell Stem Cell* **10**, 398-411.

Ma, R., Latif, R. and Davies, T. F. (2015). Human embryonic stem cells form functional thyroid follicles. *Thyroid* **25**, 455-461.

Macias, M. J., Martin-Malpartida, P. and Massague, J. (2015). Structural determinants of Smad function in TGF-beta signaling. *Trends Biochem Sci* **40**, 296-308.

Matsubara, T., Araki, M., Abe, H., Ueda, O., Jishage, K., Mima, A., Goto, C., Tominaga, T., Kinosaki, M., Kishi, S., et al. (2015). Bone Morphogenetic Protein 4 and Smad1 Mediate Extracellular Matrix Production in the Development of Diabetic Nephropathy. *Diabetes* **64**, 2978-2990.

Monteiro, R. M., de Sousa Lopes, S. M., Bialecka, M., de Boer, S., Zwijsen, A. and Mummery, C. L. (2008). Real time monitoring of BMP Smads transcriptional activity during mouse development. *Genesis* **46**, 335-346.

Morrissey, M. A. and Sherwood, D. R. (2015). An active role for basement membrane assembly and modification in tissue sculpting. *J Cell Sci* **128**, 1661-1668.

Moya, I. M., Umans, L., Maas, E., Pereira, P. N., Beets, K., Francis, A., Sents, W., Robertson, E. J., Mummery, C. L., Huylebroeck, D., et al. (2012). Stalk cell phenotype depends on integration of Notch and Smad1/5 signaling cascades. *Dev Cell* **22**, 501-514.

Nilsson, M. and Fagman, H. (2013). Mechanisms of thyroid development and dysgenesis: an analysis based on developmental stages and concurrent embryonic anatomy. *Curr Top Dev Biol* **106**, 123-170.

Petryk, A., Anderson, R. M., Jarcho, M. P., Leaf, I., Carlson, C. S., Klingensmith, J., Shawlot, W. and O'Connor, M. B. (2004). The mammalian twisted gastrulation gene functions in foregut and craniofacial development. *Dev Biol* **267**, 374-386.

Pierreux, C. E., Cordi, S., Hick, A. C., Achouri, Y., Ruiz de Almodovar, C., Prevot, P. P., Courtoy, P. J., Carmeliet, P. and Lemaigre, F. P. (2010). Epithelial: Endothelial cross-talk regulates exocrine differentiation in developing pancreas. *Dev Biol* **347**, 216-227.

Pierreux, C. E., Poll, A. V., Kemp, C. R., Clotman, F., Maestro, M. A., Cordi, S., Ferrer, J., Leyns, L., Rousseau, G. G. and Lemaigre, F. P. (2006). The transcription factor hepatocyte nuclear factor-6 controls the development of pancreatic ducts in the mouse. *Gastroenterology* **130**, 532-541.

Pohlenz, J., Maqueem, A., Cua, K., Weiss, R. E., Van Sande, J. and Refetoff, S. (1999). Improved radioimmunoassay for measurement of mouse thyrotropin in serum: strain differences in thyrotropin concentration and thyrotroph sensitivity to thyroid hormone. *Thyroid* **9**, 1265-1271.

Poschl, E., Schlotzer-Schrehardt, U., Brachvogel, B., Saito, K., Ninomiya, Y. and Mayer, U. (2004). Collagen IV is essential for basement membrane stability but dispensable for initiation of its assembly during early development. *Development* **131**, 1619-1628.

Ramasamy, S. K., Kusumbe, A. P. and Adams, R. H. (2015). Regulation of tissue morphogenesis by endothelial cell-derived signals. *Trends Cell Biol* **25**, 148-157.

Sbaa, E., Dewever, J., Martinive, P., Bouzin, C., Frerart, F., Balligand, J. L., Dessy, C. and Feron, O. (2006). Caveolin plays a central role in endothelial progenitor cell mobilization and homing in SDF-1-driven post-ischemic vasculogenesis. *Circ Res* **98**, 1219-1227.

Shao, E. S., Lin, L., Yao, Y. and Bostrom, K. I. (2009). Expression of vascular endothelial growth factor is coordinately regulated by the activin-like kinase receptors 1 and 5 in endothelial cells. *Blood* **114**, 2197-2206.

Shimizu, T., Magata, F., Abe, Y. and Miyamoto, A. (2012). Bone morphogenetic protein 4 (BMP-4) and BMP-7 induce vascular endothelial growth factor expression in bovine granulosa cells. *Anim Sci J* **83**, 663-667.

Umans, L., Vermeire, L., Francis, A., Chang, H., Huylebroeck, D. and Zwijsen, A. (2003). Generation of a floxed allele of Smad5 for cre-mediated conditional knockout in the mouse. *Genesis* **37**, 5-11.

Wang, A. Z., Ojakian, G. K. and Nelson, W. J. (1990a). Steps in the morphogenesis of a polarized epithelium. I. Uncoupling the roles of cell-cell and cell-substratum contact in establishing plasma membrane polarity in multicellular epithelial (MDCK) cysts. *J Cell Sci* **95 (Pt 1)**, 137-151.

---- (1990b). Steps in the morphogenesis of a polarized epithelium. II. Disassembly and assembly of plasma membrane domains during reversal of epithelial cell polarity in multicellular epithelial (MDCK) cysts. *J Cell Sci* **95 (Pt 1)**, 153-165.

Yurchenco, P. D. (2011). Basement membranes: cell scaffoldings and signaling platforms. *Cold Spring Harb Perspect Biol* **3**.

Figures

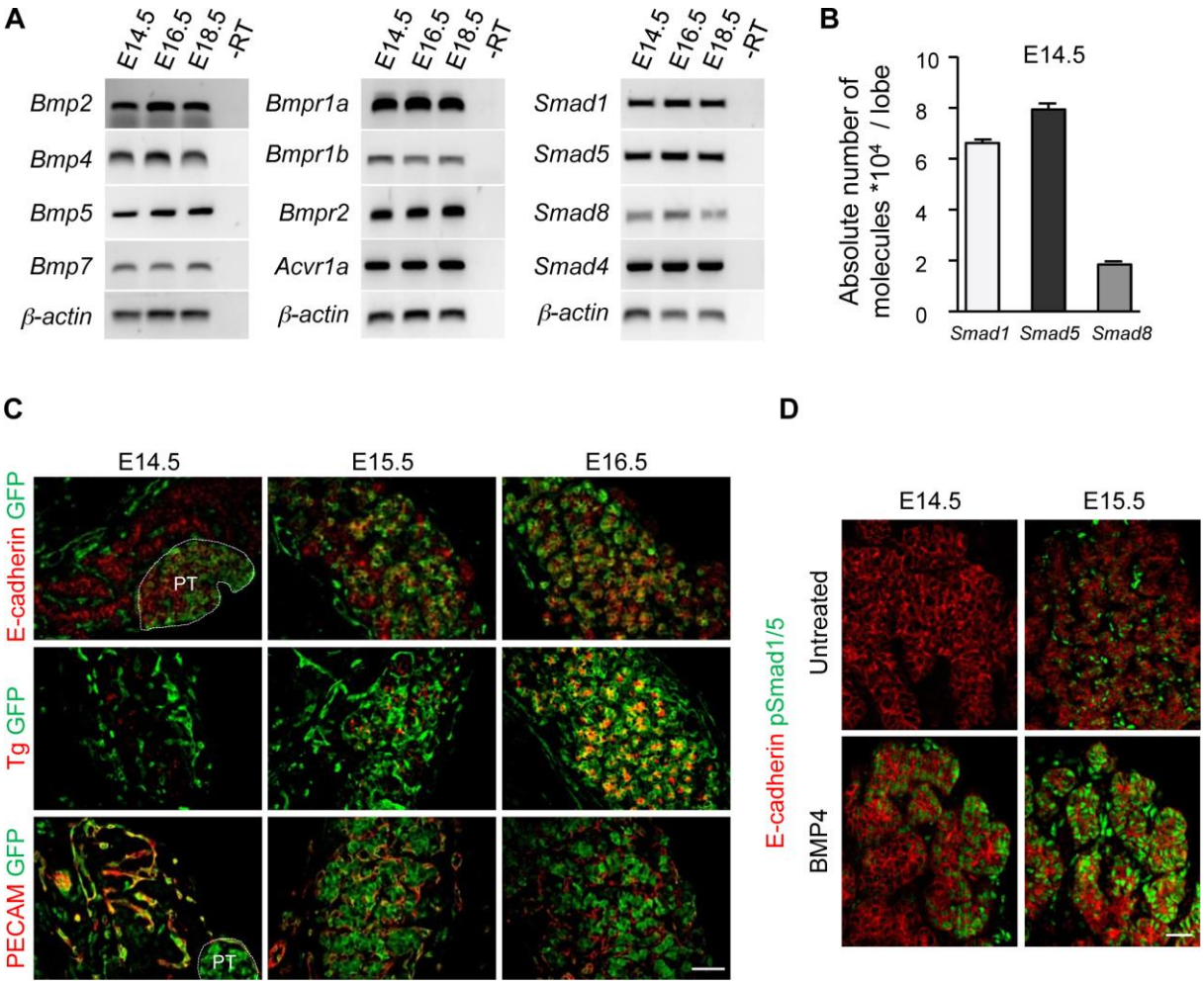

Figure 1. Active BMP signaling in thyrocyte progenitors during thyroid development. **(A)** BMP ligands, receptors and Smad intracellular mediators are expressed in the thyroid during follicle formation, from E14.5 to E18.5. *Bmp-2, -4, -5, -7* are the most abundant mRNAs in the thyroid (n≥3). **(B)** Absolute quantification of *Smad1/5/8* mRNAs at the initiation of follicle development (E14.5) reveals that Smad1 and Smad5 are the most abundant intracellular mediators of BMP signaling in the thyroid (n≥3). **(C)** Thyroid sections from BRE-GFP reporter mouse line reveal the presence of GFP (green) at E14.5 in blood vessels (PECAM, red) and parathyroid (PT, delineated by white dotted line) but not in immunolabeled thyroid epithelial cells (E-cadherin, red). From E.15.5 onwards, most

epithelial cells (thyroglobulin, red) of the developing thyroid display GFP activity. **(D)** Detection of pSmad1/5 (green) is increased on sections of E14.5 and E15.5 explants treated for 30 min with 20 ng/ml BMP4, as compared to untreated samples. Perfusion time probably explains the peripheral to central gradient of pSmad1/5. Data are presented as means ± S.E.M. Bars, (C, D) 50 μm.

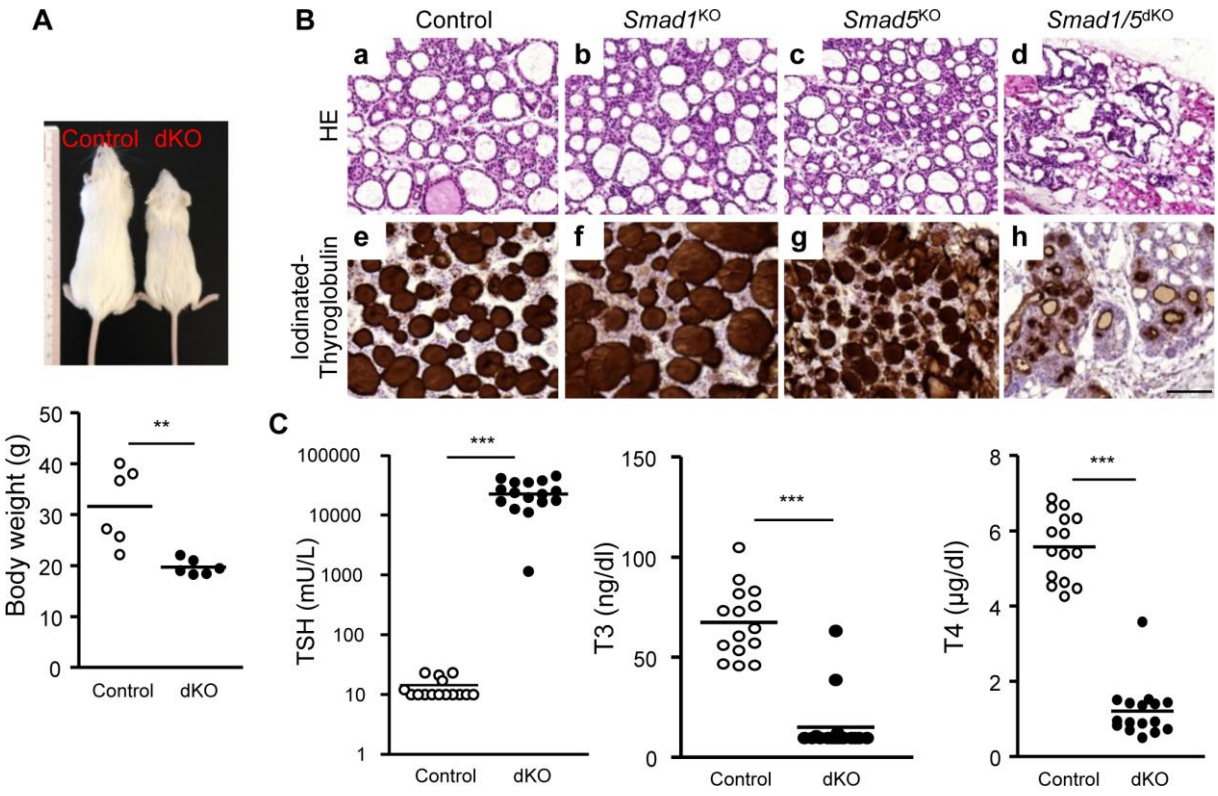

Figure 2. Smad1/5^{dKO} mice display growth retardation, abnormal follicles and hypothyroidism. Ten weeks-old single and double (d) KO mice were compared to age-matched control. **(A)** Smad1/5^{dKO} mice have smaller body size and lower body weight as compared to control. **(B)** H&E staining of control (a) Smad1^{KO} (b) and Smad5^{KO} (c) thyroids reveals abundant mature follicles lined with flat thyrocytes, while Smad1/5^{dKO} (d) thyroids exhibit severe disorganization of the thyroid parenchyma, with fewer and abnormal follicular structures lined with thicker thyrocytes suggesting high TSH level. Control (e), Smad1^{KO} (f) and Smad5^{KO} (g) thyroids show homogeneous and dense signal for iodinated-Tg in the colloid. (h) In the Smad1/5^{dKO}, iodinated-Tg is limited to a peripheral rim. **(C)** TSH, T_3 and T_4 concentrations were measured in plasma of control (open circles) and Smad1/5^{dKO} mice (filled circles) ($n \geq 15$). Most Smad1/5^{dKO} mice exhibit very high plasma or serum TSH and low T_3 and T_4. **p<0.001; ***p<0.0001 using Mann Whitney U test. Data are presented as means ± S.E.M. Bar, 100 µm.

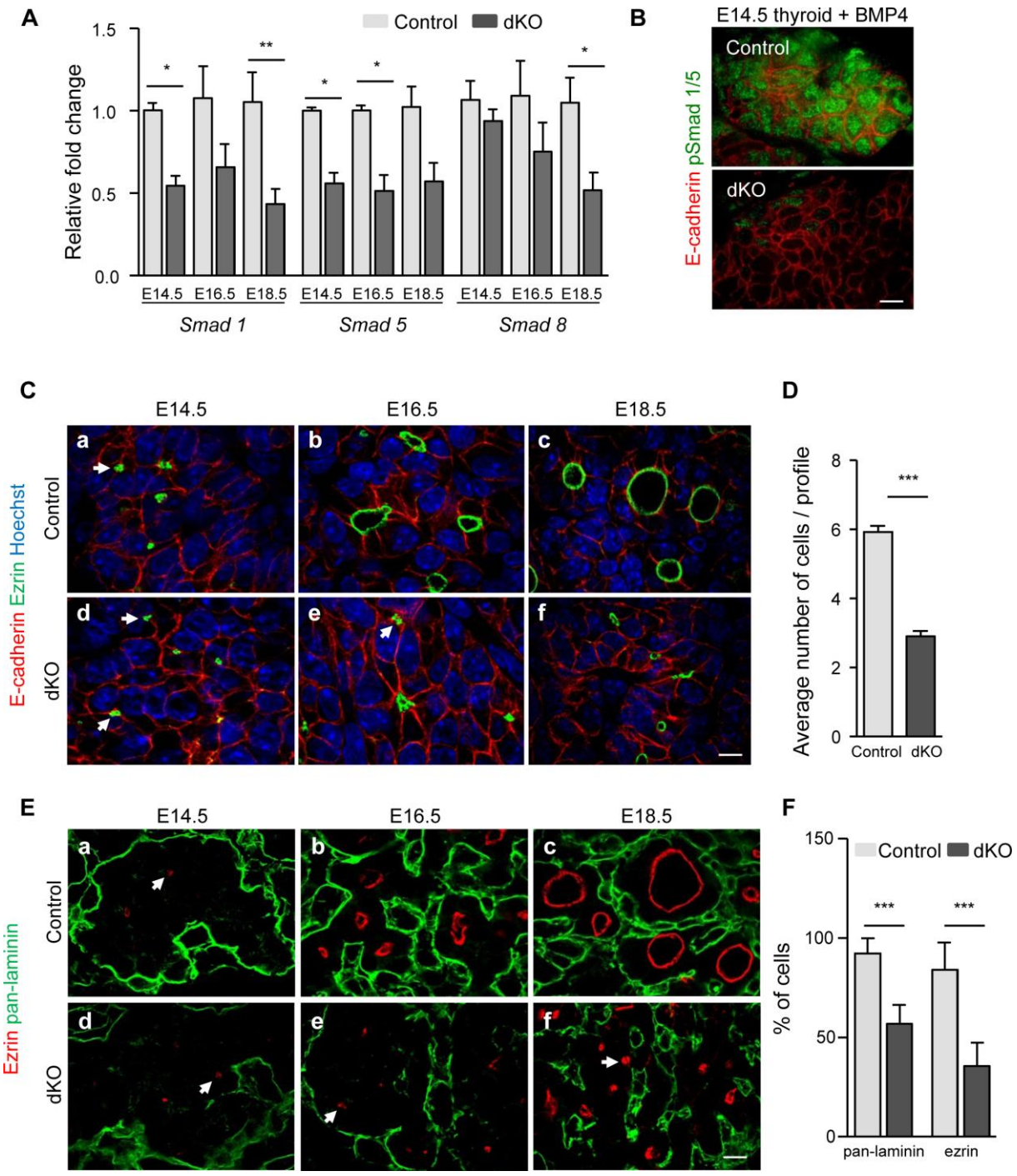

Figure 3. Smad1/5 are efficiently inactivated in thyrocyte progenitors. (A) As compared to control thyroid lobes (grey bars), Smad $1/5^{dKO}$ (black bars) show a ~50% reduction in *Smad1* and *Smad5* mRNA levels from E14.5 onwards. Expression of *Smad8* is affected at

E18.5 (n≥5). **(B)** pSmad1/5 labeling reveals Smad activation in control, but not in Smad1/5^{dKO} thyroid lobes at E14.5 treated in parallel with 20 ng/ml of BMP4. **(C)** Organization of epithelial progenitor cells (E-cadherin; red) in monolayers surrounding a lumen (ezrin; green) is impaired in Smad1/5^{dKO} thyroid glands. Arrows indicate ezrin^{+} structures in adjacent cells. **(D)** The number of cells per luminal profile of well-defined Par3^{+} structures (n≥13) is decreased by ~2-fold in thyroid glands of Smad1/5^{dKO} as compared to control. **(E)** Defective apical (ezrin; red) and basal specification (pan-laminin; green) in Smad1/5^{dKO}, as compared to control thyroid glands. Arrows indicates ezrin^{+} structures in adjacent cells. **(F)**. The number of cells in contact with pan-laminin and with ezrin is decreased in Smad1/5^{dKO}. *p<0.05; ** p<0.001; *** p<0.0001 0001 using Mann Whitney U test. All mRNAs were normalized to *RPL27*. Data are presented as means ± S.E.M. Bar, 10 μm. See also Fig. S1 in the Supplementary materials.

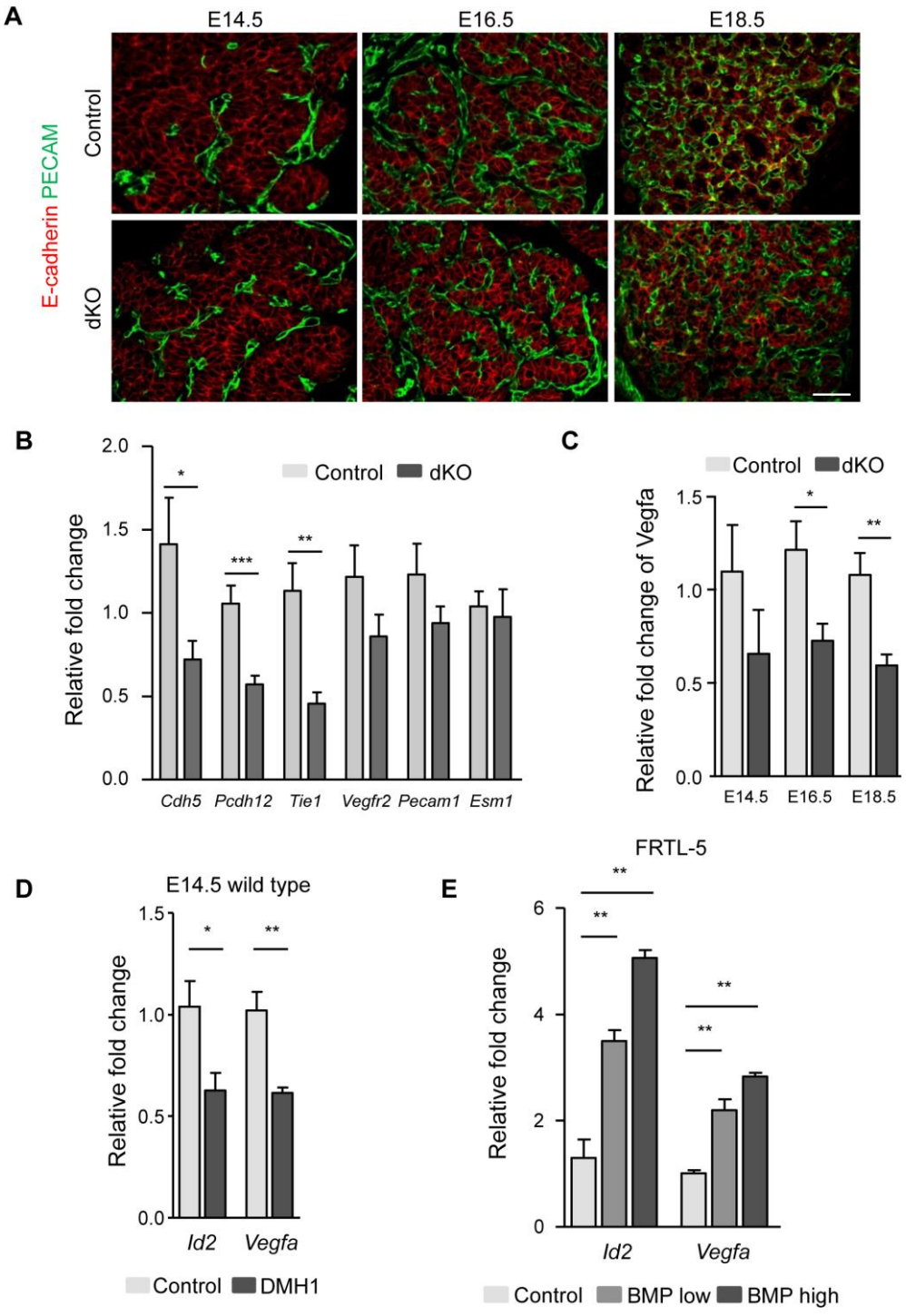

Figure 4. Normal blood vessel density but altered VEGFa and endothelial cell gene expression upon Smad1/5 inactivation. (A) Immunolabeling for E-cadherin (red) and

platelet endothelial cell adhesion molecule 1 (PECAM, green) reveals preserved blood vessel density in Smad1/5^{dKO} mice from E14.5 to E18.5. **(B)** Expression of endothelial *VE-cadherin* (*Cdh5*), *Protocadherin 12 (Pcdh12)* and *Tyrosine Kinase with Immunoglobulin-like and EGF-like domains 1 (Tie1)* are significantly reduced after epithelial inactivation of Smad1/5 at E16.5. **(C)** *Vegfa* expression is reduced in Smad 1/5^{dKO} thyroid (black bars) as compared to control (grey bars). **(D)** E14.5 thyroid lobes treated with 3 μM of the BMPR inhibitor, DMH1, for 16 hours have reduced *Id2* and *Vegfa* mRNA levels. **(E)** Expression of *Id2* and *Vegfa* in FRTL-5 cells is rapidly (8 hours) stimulated by a mix of BMP-2, -4, -5, -7 ligands in a dose-dependent manner. *$p<0.05$; ** $p<0.001$; *** $p<0.0001$ using Mann Whitney U test ($n\geq5$). All mRNAs were normalized to either *RPL27* or *β-actin*. Data are presented as means ± S.E.M. Bar, 50 μm.

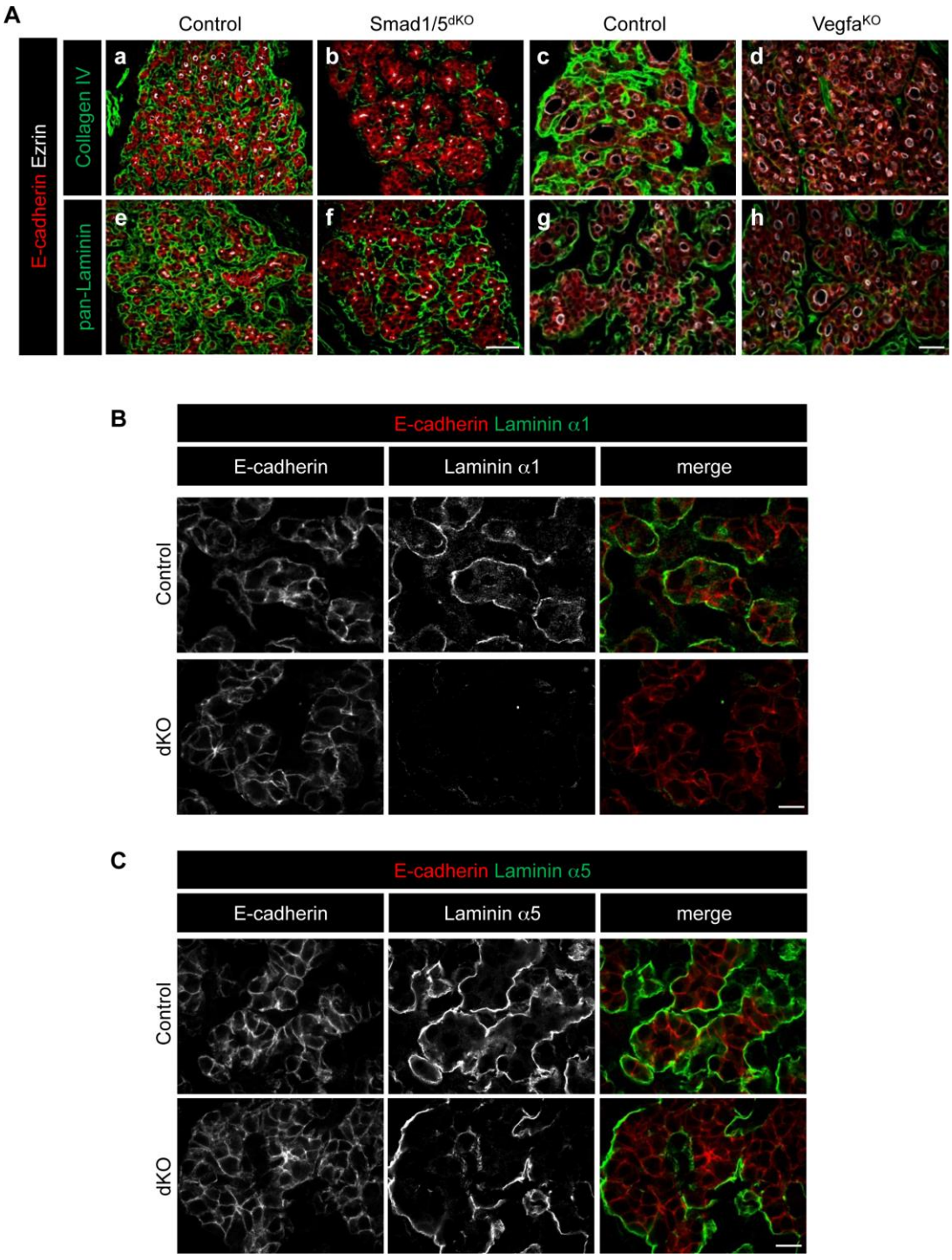

Figure 5. Production of the basement membrane proteins laminin and type IV collagen, is decreased in Smad1/5^{dKO} and Vegfa^{KO} thyroid glands. Thyroid gland sections from

Smad1/5^{dKO} at E16.5 and Vegfa^{KO} at P0 were analyzed by immunolabeling for basement membrane markers and compared to age-matched control thyroid. **(A)** Comparative multiplex immunolabeling for thyrocyte epithelial E-cadherin (red), polarity marker, ezrin (white) and basal markers, pan-laminin or type IV collagen (green). Type IV collagen signal is decreased in Smad1/5^{dKO} and Vegfa^{KO}. Pan-laminin signal shows subtle changes as compared to that in control mice. (**B**) Immunolabeling of laminin α1 (white, green), found around epithelial cells (E-cadherin; white, red) in control, is markedly decreased in Smad1/5^{dKO} at E16.5. **(C)** Immunolabelling of laminin α5 (white, green), found around epithelial cells (E-cadherin; white, red) in control is marginally affected in Smad1/5^{dKO} at E16.5. Bars, (A) 50 μm, (B, C) 10 μm. See also Fig.S2 and S3 in the Supplementary materials.

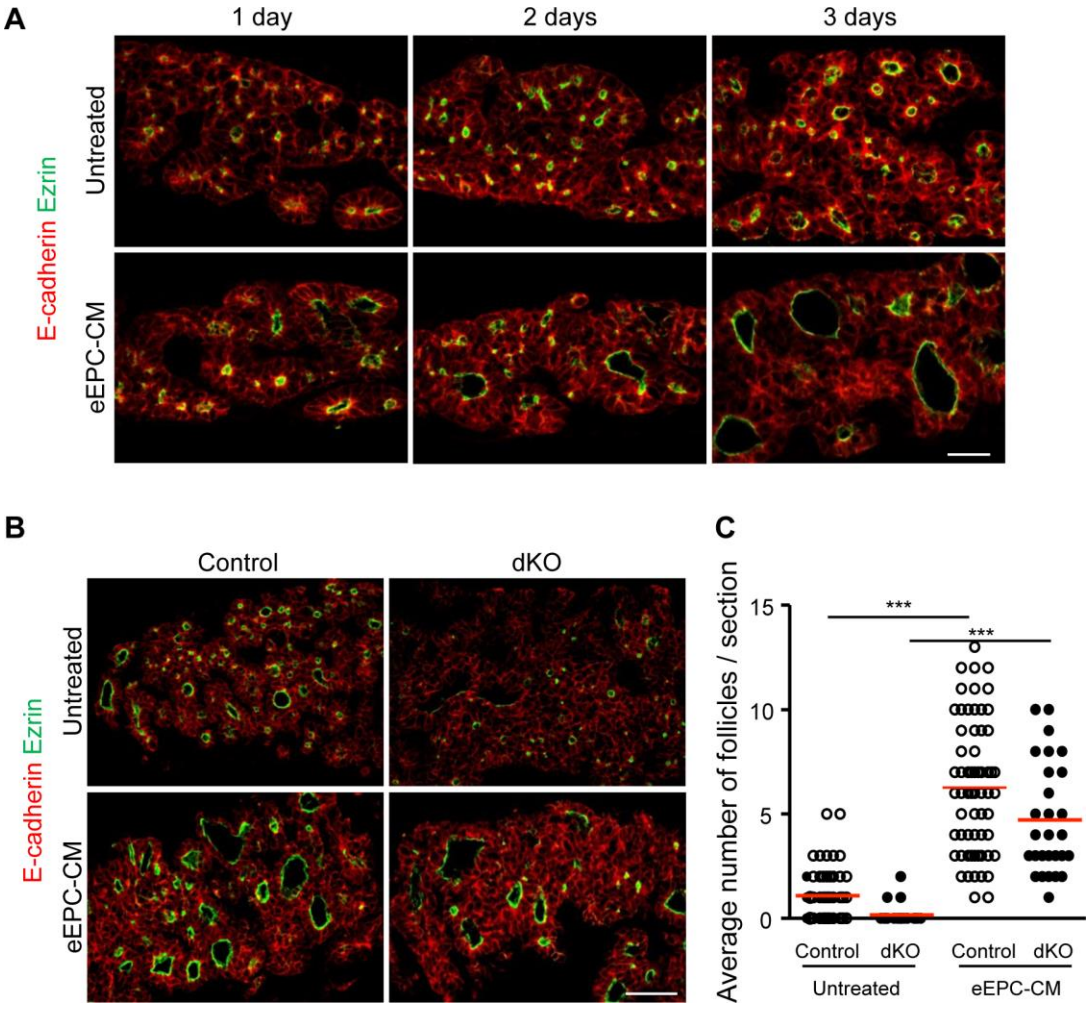

Figure 6. Medium conditioned by endothelial cells contains folliculogenic factor(s) and rescues follicle formation defect of Smad1/5^{dKO}. (A) Within 3 days of culture, epithelial cells (E-cadherin^{+}, red) from wild-type E14.5 thyroid lobes polarize apically (ezrin^{+}, green) and form small follicles. Addition of eEPC-CM to the culture stimulates polarization and follicle formation. **(B)** As compared to control, ezrin^{+} (green) structures are smaller in untreated Smad1/5^{dKO} thyroid lobes, but are enlarged when cultured with eEPC-CM. **(C)** The number of large ezrin^{+} luminal follicles per thyroid explants section was calculated. *** $p<0.0001$ using One-way ANOVA followed by Bonferroni's multiple comparison test ($n\geq23$). Data are presented as means ± S.E.M. Bars, (A) 20 μm and (B) 50 μm. See also Fig. S4 in the Supplementary materials.

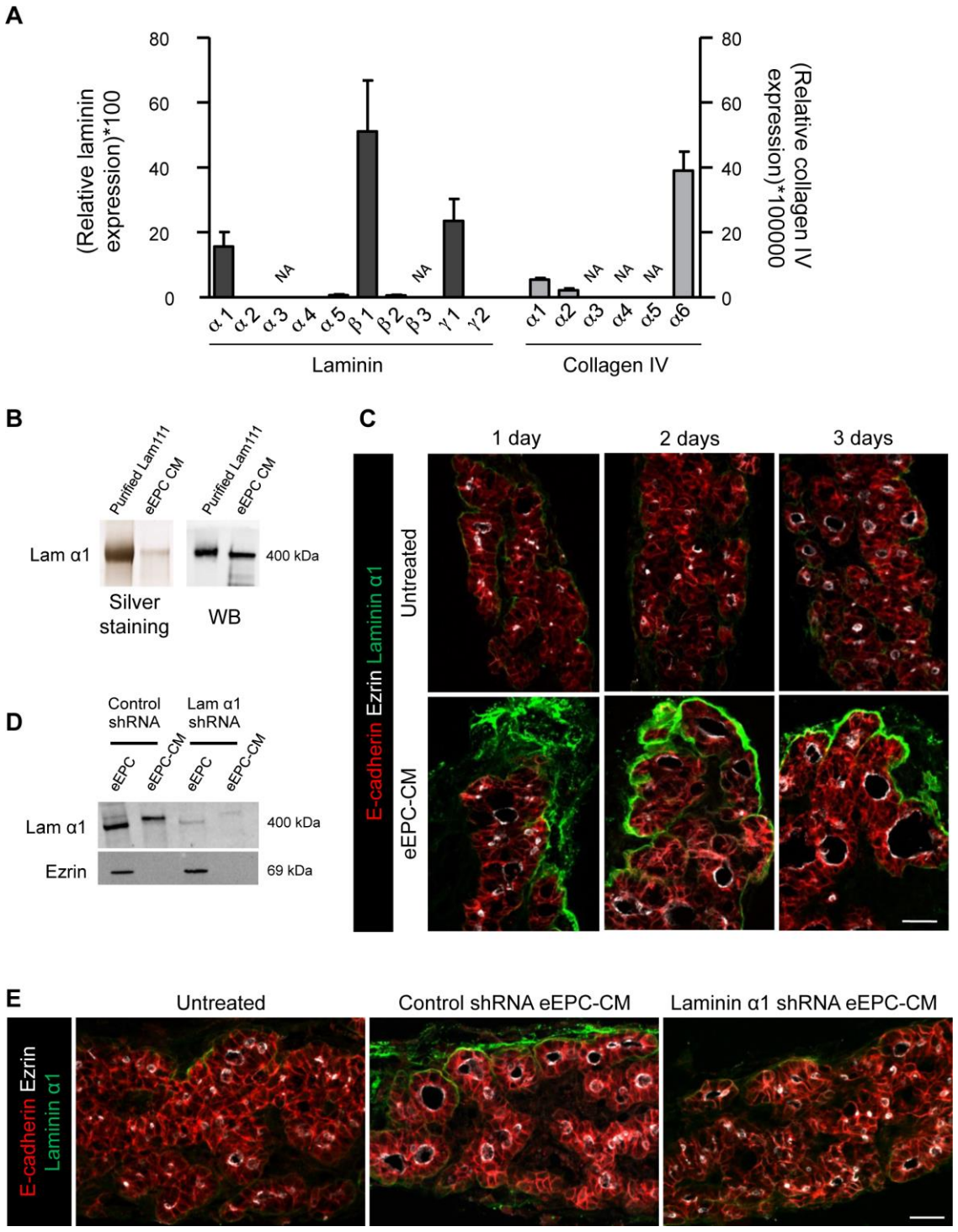

Figure 7. Laminins deposited and assembled around thyroid epithelial cells, promote folliculogenesis. (A) eEPC cells express high level of selected laminin genes and much lower

level of collagen IV genes. All mRNAs were normalized to *β-actin*. Data are presented as means ± S.E.M. (n≥3) **(B)** *Laminin α1* (400 kDa) is secreted by eEPC and accumulates in eEPC-CM. **(C)** E14.5 thyroid lobes cultured with eEPC-CM show intense signal for laminin α1 (green) around thyroid epithelial cells (E-cadherin, red), and larger follicles (ezrin, white) as compared to untreated lobes. **(D)** shRNA-mediated *laminin α1* silencing in eEPC decreases laminin α1 in eEPC extract and CM, as compared to control shRNA. Ezrin is used as a loading control for eEPC extracts. **(E)** As compared to thyroid lobes cultured with control shRNA eEPC-CM, lobes cultured in the presence of CM from *laminin α1* shRNA eEPC do not show laminin α1 deposition and have small follicles, similar to those of untreated lobes. Bar, 20 μm.